

# A Kinetic Framework for a Mammalian RNA Polymerase in Vivo

Miroslav Dundr,<sup>1</sup> Urs Hoffmann-Rohrer,<sup>2</sup> Qiyue Hu,<sup>3</sup>  
Ingrid Grummt,<sup>2</sup> Lawrence I. Rothblum,<sup>3</sup> Robert D. Phair,<sup>4</sup>  
Tom Misteli\*<sup>1</sup>

by *roX* mutations (Fig. 3, E and F). These results suggest that spreading is likely to be a general phenomenon, occurring in many or most tissues of the animal. When the MSL complex spreads over genes surrounding *roX1*, the chromatin is remodeled for increased transcription. If ectopic MSL spreading occurs in a repressive chromatin environment, even strong silencing may be overcome. The consistency of ectopic spreading correlates with increased transcription of flanking chromatin.

We have found conditions in which *roX* RNAs either assemble into MSL complexes that preferentially spread in cis from the site of transcription or diffuse to the X chromosome. We propose that these outcomes are determined by MSL proteins assembling onto growing *roX* transcripts tethered to the chromosome. The local pool of MSL proteins would control the efficiency of this process. If active complexes are completed by the time 3' RNA processing releases the RNA from the chromosome, the most likely outcome is immediate entry and spreading into flanking chromatin. If the supply of MSL subunits is reduced by a competing source of *roX* RNA, release of *roX* transcripts might precede complex maturation. These MSL complexes are unlikely to return to the transgene after assembly in solution and instead diffuse to the X chromosome, which, in addition to *roX* genes, has unknown features that make it the best target for MSL complexes.

## References and Notes

- R. E. Kingston, G. J. Narlikar, *Genes Dev.* **13**, 2339 (1999).
- A. J. Bannister *et al.*, *Nature* **410**, 120 (2001).
- J. T. Lee, R. Jaenisch, *Nature* **386**, 275 (1997).
- M. Lachner, D. O'Carroll, S. Rea, K. Mechtler, T. Jenuwein, *Nature* **410**, 116 (2001).
- J.-i. Nakayama, J. C. Rice, B. D. Strahl, D. C. Allis, S. I. S. Grewal, *Science* **292**, 110 (2001).
- Y. Ho, F. Elefant, N. Cooke, S. Liebhauer, *Mol. Cell* **9**, 291 (2002).
- R. L. Kelley *et al.*, *Cell* **98**, 513 (1999).
- J. C. Lucchesi, *Curr. Opin. Genet. Dev.* **8**, 179 (1998).
- Y. Park, M. I. Kuroda, *Science* **293**, 1083 (2001).
- Y. Wang, W. Zhang, Y. Jin, J. Johansen, K. M. Johansen, *Cell* **105**, 433 (2001).
- A. Franke, B. S. Baker, *Mol. Cell* **4**, 117 (1999).
- V. H. Meller, B. P. Rattner, *EMBO J.* **21**, 1084 (2002).
- V. H. Meller *et al.*, *Curr. Biol.* **10**, 136 (2000).
- Y. Kageyama *et al.*, *EMBO J.* **20**, 2236 (2001).
- Y. Park *et al.*, unpublished data.
- K. A. Chang, M. I. Kuroda, *Genetics* **150**, 699 (1998).
- R. A. Henry, B. Tews, X. Li, M. Scott, *J. Biol. Chem.* **276**, 31953 (2001).
- J. M. Belote, J. C. Lucchesi, *Nature* **285**, 573 (1980).
- U. Bhadra, M. Pal-Bhadra, J. A. Birchler, *Genetics* **152**, 249 (1999).
- S. Netter, M. O. Fauvarque, R. Diez del Corral, J. M. Dura, D. Coen, *Genetics* **149**, 257 (1998).
- K. W. Choi, B. Mozer, S. Benzer, *Proc. Natl. Acad. Sci. U.S.A.* **93**, 5737 (1996).
- We thank C. Stuckenholz and K. Choi for fly stocks and W. Mattox and X. Bai for critical reading of the manuscript. We thank H. Kennedy and R. Richman for excellent technical assistance. Supported by NIH grants GM45744 (M.I.K.) and GM58427 (V.H.M.), the Welch Foundation, and the Howard Hughes Medical Institute (HHMI). M.I.K. is an HHMI Investigator.

We have analyzed the kinetics of assembly and elongation of the mammalian RNA polymerase I complex on endogenous ribosomal genes in the nuclei of living cells with the use of in vivo microscopy. We show that components of the RNA polymerase I machinery are brought to ribosomal genes as distinct subunits and that assembly occurs via metastable intermediates. With the use of computational modeling of imaging data, we have determined the in vivo elongation time of the polymerase, and measurements of recruitment and incorporation frequencies show that incorporation of components into the assembling polymerase is inefficient. Our data provide a kinetic and mechanistic framework for the function of a mammalian RNA polymerase in living cells.

Within the mammalian nucleus, the tandemly repeated ribosomal genes are localized specifically in morphologically distinct nucleolar structures termed "fibrillar centers" (FCs), where they are transcribed exclusively by RNA polymerase I (1–3). FCs are naturally occurring gene arrays enriched in components of the RNA pol I machinery and are therefore an ideal system to visualize and to quantitatively study the dynamics of an RNA polymerase on its endogenous target in living cells.

In order to visualize RNA pol I in vivo, we tagged several RNA pol I components, including preinitiation factors Upstream Binding Factor 1 (UBF1), UBF2, and Transcription Associated Factor<sub>48</sub> (TAF<sub>48</sub>), assembly factors Polymerase Associated Factor 53 (PAF53) and Transcription Initiation Factor-1A (TIF-1A/Rn3), and the subunits of the polymerase (RPA194, RPA43, RPA40, and RPA 16) with the green fluorescent protein (GFP). The fusion proteins were expressed transiently or stably in CMT3 monkey kidney cells where fusion proteins accumulated in the nucleolus in multiple foci indicative of FCs (Fig. 1, A and B). The punctate sites of accumulation were confirmed to be endogenous ribosomal genes by fluorescence in situ hybridization using a specific probe against the nascent 5' External Transcribed Spacer (ETS) core segment of preribosomal RNA (pre-rRNA) (Fig. 1A) (4). Intact ribosomal

DNA (rDNA) transcription in cells expressing tagged RNA pol I components was confirmed by incorporation of 5-bromouridine 5'-triphosphate (BrUTP) in in situ run-on assays (Fig. 1B). As observed for endogenous RNA pol I components by antibody staining, a weak diffuse nucleoplasmic signal and a cytoplasmic pool was detected for all fusion proteins (Fig. 1, A and B) in addition to the strongly labeled FCs. The expected localization of the fusion proteins in nucleolar foci is consistent with their proper functioning, because GFP fusions of several nonfunctional mutants of UBF1, PAF53, and RPA194 did not accumulate in FCs and were found throughout the nucleus (5).

To test whether the GFP fusion proteins were functionally incorporated into the RNA pol I transcription complex, we transfected the fusion proteins into cells stably expressing the FLAG-tagged pol I assembly factor TIF-1A/Rn3 (6). When the RNA pol I holoenzyme was isolated by use of the FLAG epitope, GFP-tagged TAF<sub>48</sub>, TIF-1A/Rn3, PAF53, RPA194, RPA43, RPA40, and RPA16 were recovered with the holoenzyme, whereas GFP-UBF1 and GFP-UBF2 were not efficiently pulled down, confirming their weak association with the holoenzyme (Fig. 1C) (7, 8). Separate experiments confirmed that the pulled-down RNA pol I was transcriptionally active (9).

We used fluorescence recovery after photobleaching (FRAP) to study the dynamics of recruitment of RNA pol I components to endogenous ribosomal genes (Fig. 2) (10). Sites of rDNA transcription in cells expressing one of the RNA pol I fusion proteins were bleached with the use of a short laser pulse that irreversibly

<sup>1</sup>National Cancer Institute (NCI), National Institutes of Health, Bethesda, MD 20892, USA. <sup>2</sup>German Cancer Research Center, 69120 Heidelberg, Germany. <sup>3</sup>Weis Center for Research, Danville, PA 17821, USA. <sup>4</sup>Bioinformatics Services, Rockville, MD 20854, USA.

\*To whom correspondence should be addressed. E-mail: misteli@mail.nih.gov

REPORTS

quenches the GFP signal, and the recovery of signal in the bleached area was recorded by time-lapse confocal microscopy (17). As previously observed for GFP-UBF1 (12), all three preinitiation factors—GFP-UBF1, GFP-UBF2, and TAF<sub>48</sub>-GFP—recovered

within 30 to 35 s after bleaching (Fig. 2, A and B), indicating that these components are rapidly and continuously exchanged from sites of rDNA transcription and only bind transiently to ribosomal genes in FCs.

The recovery kinetics of four RNA pol I subunits, including GFP-RPA194, the largest catalytic subunit that contacts DNA, were analyzed analogously (Fig. 2, A and C). Recovery for all RPA subunits showed biphasic kinetics, with a rapid increase in fluorescence signal before reaching a second phase of slower recovery 30 to 40 s after bleaching (Fig. 2C). Whereas the initial phase of rapid recovery is indicative of a fraction that rapidly exchanges between the nucleolus and the nucleoplasm, the second phase represents subunits in elongating polymerases, because this fraction was abolished in transcriptionally inactive mitotic cells (fig. S2). The differences in the initial rates of recovery of these subunits indicate that the majority of molecules are not present in a common holoenzyme and that they are imported into the nucleolus as distinct subunits (Fig. 2C). Similar recovery kinetics were observed for the putative assembly factors GFP-PAF53 and GFP-TIF-IA/Rrn3, suggesting that they too enter the nucleolus independently of the RPA subunits (5). Recovery kinetics were independent of expression level of the fusion protein, and identical results were observed for stably or transiently expressed constructs and for CMT3, HSC, and NIH 3T3 cells (5).

In order to specifically visualize the fraction of RNA pol I subunits engaged in elongation and to obtain quantitative information about dynamics of elongation, we applied a modified bleaching method termed “iFRAP” (inverse FRAP). In iFRAP, the entire cell nucleus with the exception of a small region of interest containing a few sites of rDNA transcription is bleached (Fig. 3). In this way, a snapshot of the GFP fusion protein at sites of ribosomal gene expression at the time of bleaching is obtained. The loss of fluorescence is a direct indicator of the dissociation kinetics of a protein from ribosomal genes (Fig. 3). When iFRAP was applied to cells expressing GFP-RPA194, the major fraction of the fluorescence signal for GFP-RPA194 dropped rapidly within 5 s after bleaching, followed by a slow decrease in the fluorescence signal (Fig. 3, A and B). Similar to GFP-RPA194, all RPA subunits exhibited an initial phase of rapid loss followed by a slow, linear decline phase (Fig. 3). Consistent with the FRAP results, these kinetics suggest that the major fraction of each RNA pol I subunit is not engaged in transcription at any given time. The slow phase was confirmed to represent elongating RPA molecules because addition of the nucleotide analog cordycepin (3′-deoxyadenosine), which acts as an elongation chain terminator (13), resulted in stalling and slow dissociation of GFP-RPA194 from ri-

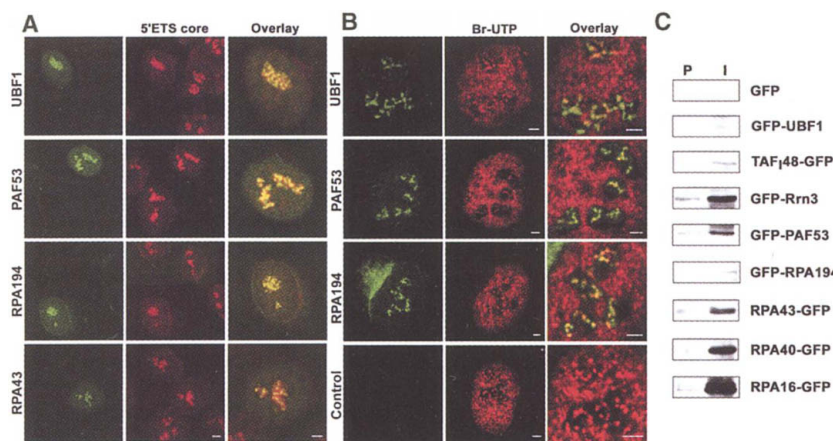


**Fig. 1.** (A) RNA pol I-GFP fusion proteins colocalize with pre-rRNA in nucleolar FCs. Ribosomal RNA was detected by fluorescence in situ hybridization with a probe to the 5'ETS of pre-rRNA (red) in CMT3 cells transfected with the indicated GFP-fusion protein (green). (B) BrUTP incorporation in FCs containing pol I-GFP fusion proteins. CMT3 cells transfected with the indicated GFP-fusion protein (green) were incubated with BrUTP for 8 min to visualize active transcription sites (red), which colocalized with GFP fusion proteins in nucleoli (yellow in overlay). (C) GFP-Pol I fusion proteins are incorporated into RNA pol I in vivo. 3T3 F5 cells stably expressing FLAG-TIF-IA/Rrn3 were transfected with GFP-pol I fusion proteins, and whole cell extracts were immunoprecipitated with antibodies to FLAG. The presence of pol I-GFP fusion proteins was probed by immunoblotting with an antibody to GFP. P, pre-immune serum; I, anti-GFP immune serum. Bars, 2  $\mu$ m; overlays, 4  $\mu$ m.

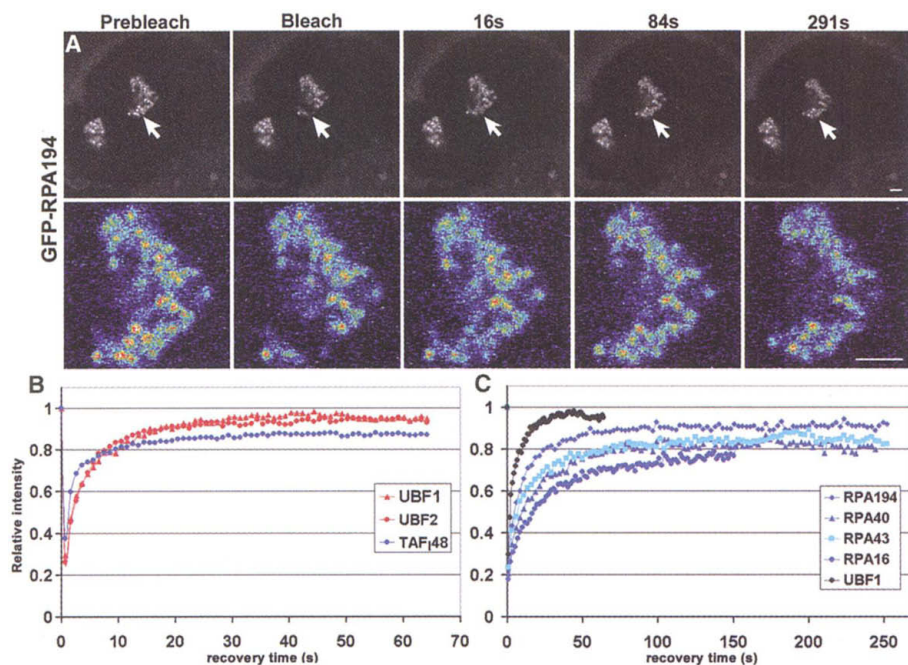


**Fig. 2.** FRAP of RNA pol I fusion proteins. (A) Cells expressing GFP-RPA194 were imaged before and after photobleaching of FCs inside of the nucleolus. The recovery of the fluorescent signal was monitored by time-lapse microscopy. The bleached area is indicated by arrows and is shown as enlarged pseudocolor panels. (B and C) Quantitation of recovery kinetics. For quantitation, at least 20 cells from at least two independent experiments were used. Bar, 2  $\mu$ m.

## REPORTS

bosomal genes (Fig. 3B). In contrast, the nonelongating GFP-UBF1 and TAF<sub>48</sub>-GFP did not exhibit any slow phase in iFRAP experiments (Fig. 3D), and they were insensitive to cordycepin (Fig. 3C). The iFRAP curves for GFP-PAF53 and GFP-TIF-IA/Rrn3 were similar to that observed for GFP-RPA194 (Fig. 3E).

To obtain quantitative information about assembly and elongation kinetics of RNA pol I components, we analyzed the iFRAP data with the use of a kinetic model based on standard principles of chemical kinetics (Fig. 4A) (14). The cycle of RNA pol I components can be described as a system of differential equations containing kinetic parameters of the pol I subunits as variables. For quantitation purposes, we assumed ~100 polymerases per active gene and a total number of active ribosomal genes of ~100 to 120 per nucleus (15–17). The known size of the elongating pool (~100 polymerases per gene) and a rough estimate of the absolute abundance of GFP-tagged molecules in FCs were used as stringent constraints for obtaining the best fits to the model (18). Least squares best fit analysis of the experimental iFRAP data allowed the extraction of several kinetic parameters for RNA pol I components (Table 1, table S1). Qualitative and quantitative analyses gave best fits for GFP-RPA194, RPA43-GFP, RPA40-GFP, and RPA16-GFP, with elongation times of 113 to 182 s and an average of 140 s (Table 1, Fig. 4B). No fits to the model for any of the RPA subunits could be obtained when we assumed that they were not incorporated into elongating RNA pol I (Fig. 4B). Similarly, GFP-PAF53 data could only be fit when assuming incorporation into elongating RNA pol I, and the best fit elongation time for GFP-PAF53 was 143 s (Table 1). In contrast, the iFRAP data for GFP-UBF1, GFP-UBF1-N-box 3, and TAF<sub>48</sub>-GFP could only be fit to a nonelongation model (Table 1). Longer or shorter elongation times, including the complete absence of elongation, could not account for the experimental data on RPAs, and a rescue of these degenerate fits by alterations of other parameters was unsuccessful (Fig. 4B). When we tested the alternative possibilities that either the initial fast or the immobile fraction represented the elongating pool of RPA subunits, we obtained unrealistic elongation times of less than 5 s and more than 5 hours, respectively.

We conclude from this analysis that the elongation phase of RNA pol I on ribosomal genes takes ~140 s, corresponding to an elongation rate of 95 nucleotides/s for a human rDNA gene of 13.3 kb (19). Given our estimated average elongation time of 140 s and about 100 polymerases on an

average gene, the reinitiation interval at a ribosomal promoter can thus be estimated to be ~1.4 s. This number is consistent with the best fit residence times of all RPA subunits on the promoter of between 0.2 and 1.2 s (Table 1). The FC residence times of GFP-UBF1 and TAF<sub>48</sub>-GFP are on the order of 3 to 5 s, allowing for the possibility that these preinitiation factors function in multiple rounds of initiation before dissociation from the nucleus (20).

An initiation rate of 1.4 s is consistent with the production of  $6 \times 10^6$  to  $8 \times 10^6$  ribosomal transcripts within 24 hours, which is the required rate of ribosome synthesis to ensure cell viability (21).

We further used the kinetic model to explore the assembly kinetics of components of RNA pol I. By comparing the exit rate from the nucleolus with the entry rate

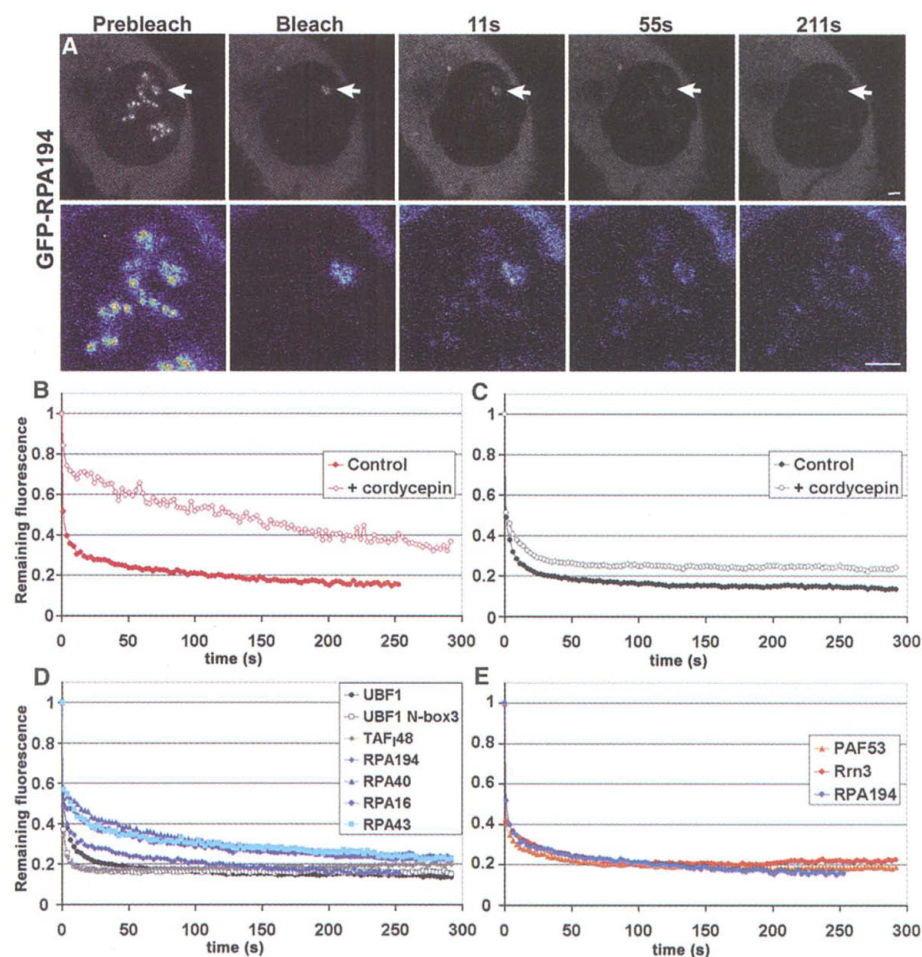


**Fig. 3.** iFRAP of RNA pol I fusion proteins. (A) Cells expressing GFP-RPA194 were imaged before and after photobleaching of the entire nucleus, with the exception of a few FCs inside of the nucleolus. The loss of fluorescent signal was monitored using time-lapse microscopy. The unbleached area monitored is indicated by arrows and is shown as enlarged pseudocolor panels. (B to E) Quantitation of iFRAP kinetics. Bar, 2  $\mu$ m.

**Table 1.** Kinetic parameters for RNA pol I components. Plus signs, elongating subunit. Minus signs, nonelongating subunit. N/A, not applicable.

	Elongating	Residence time(s)		Probability	
		Elongation	Promoter	Promoter	Initiation
UBF1	–	N/A	0.16	0.56	0.0045
UBF1 N-box3	–	N/A	0.16	0.14	0.0042
TAF <sub>48</sub>	–	N/A	0.34	0.52	0.0035
PAF53	+	143	0.17	0.50	0.010
RPA194	+	143	0.17	0.44	0.012
RPA43	+	181	0.46	0.59	0.025
RPA40	+	113	0.54	0.58	0.047
RPA16	+	120	1.37	0.34	0.114

## REPORTS

onto the promoter [ $k_{\text{on}}/(k_{\text{on}} + k_r)$ ] (Fig. 4A), we determined the probability of an RNA pol I component that has entered the nucleolus to associate with a ribosomal promoter. A least squares best fit analysis resulted in a promoter recruitment probability of  $\sim 50\%$  for all subunits (Table 1). As a control, the UBF1N-box 3 mutant showed a considerably lower promoter probability (Table 1), consistent with its ability to recognize the rDNA promoter but its inability to interact with other RNA pol I components (15).

We next determined the efficiency of incorporation of RNA pol I subunits into an elongation-competent holoenzyme at the ribosomal promoter by comparing their promoter entry rates with their promoter exit rates [ $k_{\text{start}}/(k_{\text{start}} + k_{\text{off}})$ ] (Fig. 4A). Best fit analyses indicate that the efficiency of incorporation of RNA pol I components into an elongation-competent complex is low for all subunits. Initiation probabilities ranged from 1% for GFP-RPA194 to 11% for RPA16-GFP (Table 1). As expected, the efficiencies of incorporation of the non-elongating GFP-UBF1 and TAF<sub>48</sub>-GFP were an order of magnitude lower than for elongating subunits and were well within the experimental error of our measurements (Table 1). Sensitivity analysis of initiation probabilities showed that probabilities of up to 0.2 resulted in degraded fits and that initiation probabilities greater than 0.2 were entirely inconsistent with our experimental data (10). Taken together, these observations suggest that although the association of an

RNA pol I component with a ribosomal gene promoter is a frequent event, its incorporation into an elongating polymerase is inefficient.

Our results provide a kinetic framework for RNA pol I transcription *in vivo*. We find that the RNA pol I machinery is a highly dynamic protein complex. RNA pol I components are steadily and rapidly exchanged between the nucleoplasm and ribosomal transcription sites in the nucleolus, and we show that RNA pol I subunits enter the nucleolus as distinct subunits rather than as a preassembled holoenzyme. Our data suggest that on average several thousand molecules of each subunit pass through the nucleolus per second and that the residence times of all RNA pol I components in the nucleolus are on the order of seconds if they are not incorporated into an elongating complex. The fraction of RPA subunits engaged on ribosomal genes is small (7 to 10%), and the vast majority of RNA pol I subunits are not engaged in elongation at any given time. The observed rapid exchange of more than 95% of the pool of each protein between the FCs and the nucleoplasm suggests that RNA pol I machineries are not recycled, but that they reassemble at each round of transcription (22).

We find that the assembly of the RNA pol I machinery is a highly inefficient event *in vivo*. Although "capture" of RNA pol I components is efficient ( $\sim 50\%$ ), the successful formation of an elongating complex is inefficient and probably rate-limiting. Our observation that the incorporation ef-

iciency of RPA40-GFP and RPA16-GFP, which are unable to bind DNA by themselves, are higher than that of the other subunits suggests that these molecules join the assembling complex at a late stage. In contrast, GFP-RPA194 has the lowest incorporation frequency of all subunits tested, consistent with the proposal that the largest subunit joins the preinitiation factors and assembly factors relatively early and then acts as a nucleation site for assembly of the full holoenzyme (22, 23). These observations suggest that RNA pol I assembly may proceed in a sequential manner via metastable intermediates, each with increasing stability as more subunits are added. It remains to be determined whether this probabilistic assembly process is unique to RNA polymerase I or is a general feature of polymerases and macromolecular machines.

### References and Notes

1. M. R. Paule, R. J. White, *Nucleic Acids Res.* **28**, 1283 (2000).
2. P. J. Shaw, E. G. Jordan, *Annu. Rev. Cell Dev. Biol.* **11**, 93 (1995).
3. M. Carmo-Fonseca, L. Mendes-Soares, I. Campos, *Nature Cell Biol.* **2**, E107 (2000).
4. M. Dunder, T. Misteli, M. O. Olson, *J. Cell Biol.* **150**, 433 (2000).
5. M. Dunder, unpublished observation.
6. A. H. Cavanaugh *et al.*, *J. Biol. Chem.* (2002).
7. I. Grummt, *Prog. Nucleic Acid Res. Mol. Biol.* **62**, 109 (1999).
8. R. D. Hannan, A. Cavanaugh, W. M. Hempel, T. Moss, L. Rothblum, *Nucleic Acids Res.* **27**, 3720 (1999).
9. I. Grummt, L. Rothblum, unpublished observations.
10. Materials and methods are available as supporting material on Science Online.
11. R. D. Phair, T. Misteli, *Nature* **404**, 604 (2000).
12. D. Chen, S. Huang, *J. Cell Biol.* **153**, 169 (2001).
13. M. Zeevi, J. R. Nevins, J. E. Darnell Jr., *Mol. Cell Biol.* **2**, 517 (1982).
14. R. D. Phair, T. Misteli, *Nature Rev. Mol. Cell Biol.* **2**, 898 (2001).
15. O. L. Miller Jr., A. H. Bakken, *Acta Endocrinol. Suppl.* **168**, 155 (1972).
16. T. Haaf, D. L. Hayman, M. Schmid, *Exp. Cell Res.* **193**, 78 (1991).
17. U. Scheer, B. Xia, H. Merkert, D. Weisenberger, *Chromosoma* **105**, 470 (1997).
18. M. Dunder *et al.*, *J. Struct. Biol.*, in press.
19. I. L. Gonzalez, J. E. Sylvester, *Genomics* **27**, 320 (1995).
20. K. I. Panov, J. K. Friedrich, J. C. Zomerdijk, *Mol. Cell Biol.* **21**, 2641 (2001).
21. J. D. Lewis, D. Tollervey, *Science* **288**, 1385 (2000).
22. P. Aprikian, B. Moorefield, R. H. Reeder, *Mol. Cell Biol.* **21**, 4847 (2001).
23. A. Schnapp, I. Grummt, *J. Biol. Chem.* **266**, 24588 (1991).
24. We thank S. Huang, R. Intine, M. F. O'Donohue, D. Ploton, M. Olson, and R. Reeder for providing reagents and T. Karpova for technical support. Imaging was performed at the NCI Fluorescence Imaging Facility.

### Supporting Online Material

www.sciencemag.org/cgi/content/full/298/5598/1623/DC1

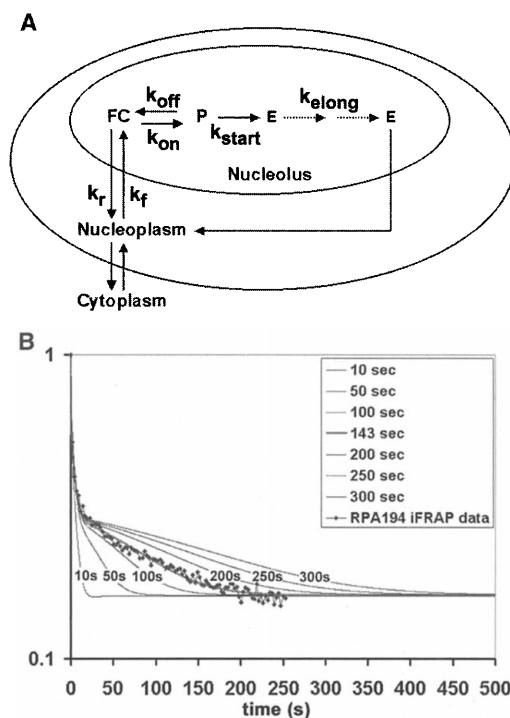
Materials and Methods

Figs. S1 and S2

Table S1

References and Notes

**Fig. 4.** Kinetic modeling of pol I assembly and elongation. **(A)** Kinetic model of RNA pol I kinetics.  $k_r$ , nucleolar dissociation rate;  $k_f$ , nuclear association rate;  $k_{\text{off}}$ , promoter off rate;  $k_{\text{on}}$ , promoter on rate;  $k_{\text{start}}$ , elongation entry rate; and  $k_{\text{elong}}$ , elongation rate. **(B)** Sensitivity analysis of the least-squares best-fit of GFP-RPA194 by altering elongation time.



15 July 2002; accepted 25 September 2002